Magnetic properties of few nanometers ε-Fe$_2$O$_3$ nanoparticles supported on the silica

S. S. Yakushkin, A. A. Dubrovskiy, D. A. Balaev, K. A. Shaykhutdinov, G. A. Bukhtiyarova, and O. N. Martyanov

View Online   Export Citation

ARTICLES YOU MAY BE INTERESTED IN

AIP Publishing

Magnetic properties of few nanometers ε-Fe$_2$O$_3$ nanoparticles supported on the silica

S. S. Yakushkin,[1,a)] A. A. Dubrovskiy,[2] D. A. Balaev,[2] K. A. Shaykhutdinov,[2] G. A. Bukhtiyarova,[1] and O. N. Martyanov[1]

[1]*Boreskov Institute of Catalysis, Russian Academy of Sciences, Siberian Branch, Novosibirsk, 630090 Russia*
[2]*Kirensky Institute of Physics, Russian Academy of Sciences, Siberian Branch, Krasnoyarsk, 660036 Russia*

Magnetic properties of ε-Fe$_2$O$_3$ nanoparticles supported on silica with the average size of few nanometers, narrow size distribution and no admixture of any other iron oxide polymorphs are investigated. The investigation of the temperature behavior of magnetization within the temperature range from 4.2 to 1000 K revealed the presence of several magnetic subsystems in the species under study. The temperatures' behavior of the magnetic moment value indicates ferrimagnetic ordering in the ε-Fe$_2$O$_3$ nanoparticles with a Curie temperature of about 800 K and points to the existence of a significant paramagnetic contribution becoming apparent at low temperatures. According to the electron spin resonance data, the particles possess superparamagnetic behavior at temperature higher ~120 K. The model of the magnetic structure of monophase system of few nanometers ε-Fe$_2$O$_3$ nanoparticles supported on silica is proposed. © *2012 American Institute of Physics*. [doi:10.1063/1.3686647]

INTRODUCTION

Manifestation of new properties with decreasing size of particles is one of the key factors governing the development of nanotechnologies. It is well known that the nanosized particles possess the magnetic properties atypical those of bulk materials and useful for applications in chemistry, biology, and medicine.[1] In particular, the superparamagnetic behavior of nanoparticles make them attractive for biomedicine because superparamagnetic nanoparticles do not form agglomerates at room temperature.[1,2] For example a porous hollow iron oxide nanoparticle system is used for controlled drug delivery and hypothermal cancer therapy.[3] However, successful application of the magnetic nanoparticles is highly dependent not only on the possibility of designing the particles with specified size and shape distribution but also on their structural uniformity that provides required magnetic properties and stability under a certain reaction conditions.

Among other magnetic nanoparticles, iron based systems are apparently one of the most available, cheap, and nontoxic magnetic materials that can be used in different applications. A number of different classes of iron-based nanoparticles are researched. Among them are core-shell particles,[4,5] which can combine a ferromagnetic core with a chemical active shell, hollow nanoparticles, a useful lightweight structural material for a wide range of applications,[6] various self-assembled arrays,[7,8] and films.[9] Iron-oxide based systems, despite not being the most sophisticated, may reveal unconventional properties[10] and as well may serve as a well-known model system with controlled size and shape[11] for any methodological work.[12] The problem of the iron oxide nanoparticles synthesis with narrow size distribution lies in the low thermal stability of the magnetic phases—FeO,

Fe$_3$O$_4$, γ-Fe$_2$O$_3$, which tend to agglomerate and quite easily transform into the antiferromagnetic oxide α-Fe$_2$O$_3$.[11] New opportunities arose recently after the way for reproducible synthesis of ε-Fe$_2$O$_3$ nanoparticles was found. The ε-Fe$_2$O$_3$ phase was mentioned for the first time in 1934;[13] this material was characterized, however, only in 1998.[14]

The magnetic properties of ε-Fe$_2$O$_3$ are intriguing. This phase is distinguished from other iron oxide polymorphs by a very high, up to H$_C$ = 20 kOe, coercivity value at room temperature[4,6,15–18] that makes ε-Fe$_2$O$_3$ a promising candidate for various applications. Otherwise, the ε-Fe$_2$O$_3$ polymorph is a collinear ferrimagnet with a Curie temperature of about 500 K; while at a temperature of approximately 110 K, it undergoes a second-order phase transition to an incommensurate magnetic structure, which results in a steep decrease in magnetization below 110 K.[15,16,19] The drop of the magnetocrystalline anisotropy is observed at 110 K along with a strong reduction of the spin-orbit coupling evidenced by a sharp decrease in orbital moment m$_{orb}$. Recently, it has been shown that such a behavior originates from the variation in the electron transfer between Fe and O ions accompanied by significant modifications of some Fe-O bond distances.[20] In a study,[18] a temperature-independent variation in the magnetic structure of ε-Fe$_2$O$_3$ was reported; with decreasing temperature, the magnetic structure of a collinear ferrimagnet changes for the square-wave incommensurate structure.

Despite the great number of experimental works, so far nobody has proposed a noncontradictory model that would explain the entire set of the magnetic phenomena observed in the ε-Fe$_2$O$_3$-based systems. Being the intermediate phase between hematite and maghemite, ε-Fe$_2$O$_3$ is stable only in nanoscale,[14,21] which makes the synthesis of a monophase system on the basis of ε-Fe$_2$O$_3$ a nontrivial task. In our opinion, the absence of such a model originates from the fact that various preparation methods used by researches may yield different size and shape distributions of the deposited

---

a)Author to whom correspondence should be addressed. Electronic mail: stas-yk@catalysis.ru.

ε-Fe_2O_3 particles as well as the presence of other iron oxide polymorphs. The magnetic properties of the particles in nanometer scale strongly depend on their size also because of a large fraction of surface atoms. It implies the surface state of the ε-Fe_2O_3 nanoparticles considerably affects their structure and magnetic properties.

Stabilization of iron-bearing particles on a substrate prevents their agglomeration and makes it possible to obtain a narrow size distribution. Recently we report a rather facile approach to synthesize the ε-Fe_2O_3 particles supported on silica with the mean size of few nanometers, narrow size distribution, and no admixture of any other iron oxide polymorphs.[22,23] The facile synthesis is based on the pore filling impregnation method by iron sulfate (II) water solution with the following annealing procedure at $\sim$1173 K. It is shown that the ε-Fe_2O_3 nanoparticles obtained are stable up to $\sim$1173 K. The monophase system based on such small ε-Fe_2O_3 particles was obtained for the first time and seemed to be the promising object for both applications and fundamental study on the structure and magnetic properties of the ε-Fe_2O_3 particles on the nanometer scale.

In this work, the magnetic properties of these ε-Fe_2O_3 particles supported on silica with the mean size of $\sim$4 nm and no admixture of any other iron oxide polymorphs are investigated. The magnetic properties of the monophase ε-Fe_2O_3 few nanometers particles system were studied for the first time. The data obtained gave grounds to proposing a model of the magnetic structure of the ε-Fe_2O_3 nanoparticles supported on silica surface.

EXPERIMENTAL

Samples were reproducibly prepared by the wet chemical pore filling impregnation method with the Fe(II) sulfate as precursors. As a carrier, KSKG silica (ChemAnalyt, state standard 3956-76) with a specific surface of 287 m^2/g, an average pore radius of $\sim$141 Å, and a pore volume of $\sim$0.35 cm^3/g was used. The grain size was within 0.25–0.5 mm.

Water solution of Fe(II) sulfate (ACS, 99 + %, CAS 7782-63-0) with contents of iron ions of 0.081 was introduced into silica hosts and dried at 383 K for 4 h. The respective approximate concentrations of iron ions for the sample were 3.4% w/v. The dried samples were calcined in air at a temperature of 1173 K for 4 h.

High-resolution transmission electron microscopic (HRTEM) images were obtained on a JEOL JEM-2010 microscope at an accelerating voltage of 200 kV with resolution of 1.4 Å. The size distribution of the nanoparticles was calculated by several photographs made in different areas of the sample. The x-ray diffraction analysis (XRD) was performed using a XTRA powder diffractometer (Switzerland) in CuK_α radiation (the wavelength is $\lambda = 1.5418$ Å) with a scanning step of 0.050 by 2θ and an accumulation time of 3 s.

Electron spin resonance (ESR) spectra were obtained on a Bruker ELEXSYS 500 radiospectrometer equipped with an ER4114HT cell, which allows operating at temperatures up to 1273 K.

Magnetization of the samples was measured using a vibrational magnetometer with the temperature range of

4.2–300 K and a PPMS-6000 facility (Quantum Design) with the temperature range of 300–1000 K.

RESULTS AND DISCUSSION

Recently it was shown that the synthesis route described in the preceding text allows one to get the system of ε-Fe_2O_3 nanoparticles supported on the silica with the mean size of few nanometers and no admixture of any other iron oxide polymorphs.[23] The size distribution of the particles estimated from the high-resolution microscopy data is rather narrow with the mean size of about 3.7 nm and standard deviation of 2.3 nm. However, as it can be seen from the particle size distribution (Fig. 1), the sample contains a small quantity of iron-oxide particles with larger size, which can be detected in MS experiments as ferromagnetic ones.

Indeed Mossbauer spectroscopic studies reveal the formation of the magnetically ordered ε-Fe_2O_3 particles after calcining the sample at temperatures above 773 K.[22] At this temperature, a drastic decrease of the chemical shift, which comes close to the values characteristic for the iron oxide, suggests the transformation of the sulfate into the ε-Fe_2O_3.[23] After calcination at 873 K, the material loses the whole of the sulfur, and sextets appear on the spectrum that correspond to the magnetic nanoparticles that appear. In addition, the paramagnetic part of the spectrum consists of the three doublets attributed to the octahedral coordination and one doublet attributed to tetrahedral one according to the isomer shifts. The Mossbauer spectra parameters allow us to refer the magnetically ordered phase to the ε-Fe_2O_3 iron oxide. At 1173 K, the fraction of the magnetically ordered phase according to the Mossbauer spectroscopy data amounts to 70% of the total Fe content in the system. The simultaneous observation in MS spectra of a ferromagnetic (sextet) and paramagnetic or superparamagnetic (doublet) state is probably due to the 30% of iron in the sample associating with
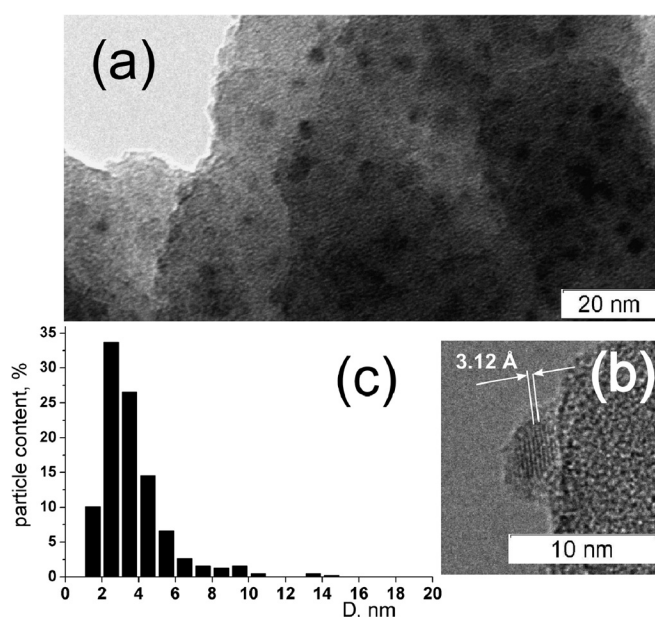
FIG. 1. (a) and (b) HRTEM images of the sample. (c) The size distributions function for the ε-Fe_2O_3 particle on the silica support estimated from the microscopy data.

the smallest superparamagnetic particles and/or to the paramagnetic ions. The comprehensive analysis of Mossbauer spectroscopy data could be found in Ref. 22.

According to the results of the magnetic measurements, with an increase in calcination temperature above 773 K, the magnetic moment grows and becomes maximum at a calcination temperature of 1173 K. The high-resolution transmission electron microscopy of the sample yields the narrow size distribution with an average size of about 3.7 nm and a mean-square deviation of 2.3 nm.

Figure 2 shows the temperature dependences of magnetization for the sample in the fields H = 1 (a), 5 (b), and 10 kOe (c) upon zero-field cooling (zfc) and cooling in a field (fc). Hereinafter, the experimental data on magnetization are given in emu divided by mass of Fe_2O_3 in the sample. It can be seen that in the low-temperature region, the values of magnetization are lower in the case of zero-field cooling. In the external field H = 1 kOe, there is the magnetization maximum at the temperature T ≈ 120 K. The temperature at which the M(T) zfc and M(T) fc start diverging (≈110 K) is close to the temperature of the M(T) maximum. With an increase in the magnetic field from 5 to 10 kOe, the M(T) zfc and M(T) fc dependences diverge already at T ≈ 75 K, and the maximum of the M(T) dependence becomes less pronounced, i.e., in the vicinity of this temperature (≈75 K), the curvature of the M(T) dependence changes its sign. The observed divergence of the M(T) zfc and M(T) fc dependences in the low-temperature region indicates the presence of superparamagnetic particles; the maximum of the M(T) dependence corresponds to the blocking temperature. The less pronounced peak at 25 K in M(T) zfc dependence can be caused by size effect due to the blocking temperature depending on the size of particles. The peak at 25 K can be attributed to the blocking temperature for smaller particles while the pronounced peak at 110 K is associated with the larger ones.

The temperature behavior of magnetization in the low-temperature region suggests that there are two magnetic subsystems (phases) with different magnetic order, superparamag-

netic and paramagnetic, in the sample. The superparamagnetic phase is characterized by the divergent M(T) fc and M(T) zfc curves below the blocking temperature, whereas the presence of the paramagnetic phase explains the M(T) fc growth at T < 50 K. In external magnetic fields of 5 and 10 kOe, the relative contribution of the paramagnetic phase increases. As a result, in the low-temperature region, magnetization grows with decreasing temperature even upon zero-field cooling. The maximum of the M(T) dependence corresponding to the blocking temperature becomes less pronounced. Analysis of the data for H = 5 and 10 kOe shows that within the range 4.2 ÷ 50 K the M(T) fc dependences are described fairly well by the expression $M(T) = A_1/T + A_2$. Thus one may conclude that, apart from the superparamagnetic particles the contribution of which at low temperature upon fc can be evaluated by constant A_2, there is the paramagnetic phase in the sample, and the contribution of this phase rapidly decreases with increasing temperature. So the dip in M(T) fc dependence below peak at 120 K can originate from paramagnetic subsystem that becomes more apparent with the increase of magnetic field. At the same time, one cannot exclude dipolar interactions between nanoparticles that in spite of relatively low iron-oxide particles content may appear in magnetization curve.

The paramagnetic contribution can be seen also in the field dependences of magnetization (M(H)) at different temperatures below the blocking temperature (Fig. 3). Indeed, at T = 65 K, the M(H) dependence is typical of the superparamagnetic particles, i.e., the dependence sharply grows in the fields of several kOe and tends to saturation in high fields, while with decreasing temperature, the paramagnetic contribution becomes more evident (Fig. 3). In the low-temperature region, the M(H) dependence is characterized by hysteresis. At the temperature T = 4.2 K, the value of coercivity is $H_c \sim 2.5$ kOe, which is considerably lower than the value known for larger ~25 nm ε-Fe_2O_3 particles.[16] The saturation magnetization values obtained are close to the ones reported in.[15,16,18,24] At the temperature T = 65 K, the hysteresis narrows to the value $H_c \sim 0.1$ kOe reflecting the approach to the

FIG. 2. Temperature dependences of the magnetic moment for the sample in different external fields and the fc and zfc regimes.
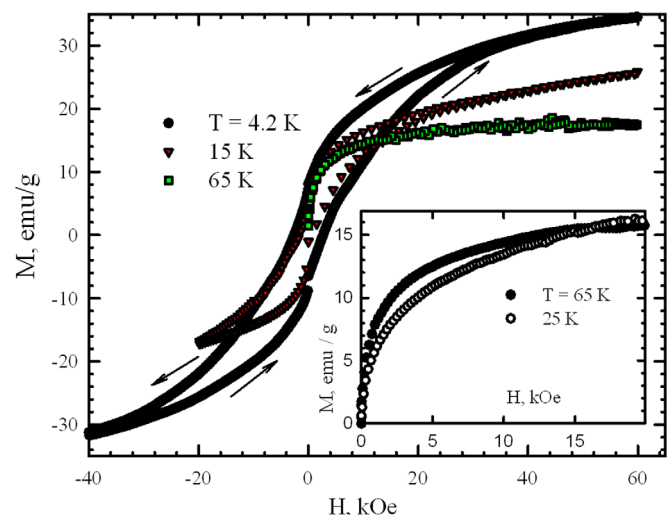
FIG. 3. (Color online) Field dependences of the magnetic moment for the sample at different temperatures. Arrows indicate the direction of variation in the external field. The insert shows the low-field path of the M(H) dependences at 25 K and 65 K.

blocking temperature. So the temperature behavior of H_c is quite close to the one reported by M. Gish,[16] while the decrease of the H_c absolute values is observed for the 4 nm ε-Fe_2O_3 particles that can be evoked by a smaller size and higher percentage of surface atoms.

The temperature evolution of the ESR spectra confirms the presence of the superparamagnetic particles in the sample (Fig. 4(a)). At high temperatures of recording, a narrow line is observed. The line shape is typical for superparamagnetic particles.[25] With temperature decrease to 120 K, the absorption line sharply broadens to 300 Oe (Fig. 4(b)), which corresponds to the blocking temperature and freezing the thermal fluctuations of the magnetic moments of a majority of the superparamagnetic particles in the sample. At 570 K, the line width is minimum (50 Oe) and remains such with a further increase in temperature. Thus at the temperature T = 570 K, which is higher than the blocking temperature by a factor of approximately 5, the fluctuations of the magnetic moment of the largest particles are defrosted, and these particles transfer to the superparamagnetic state. Because the anisotropy energy is proportional to the particle volume, the estimated maximum size of a particle is ~1.35 of the average one. Therefore the size distribution of the superparamagnetic particles in the sample is sufficiently narrow with a characteristic width of ~50% of the average particle size, which is consistent with the HRTEM data. As the temperature of spectra recording increases to 870 K, the intensity of the absorption line sharply decreases (Fig. 4(c)), which may be attributed to disappearance of the magnetic order in the ε-Fe_2O_3 nanoparticles.

Figure 5 shows the temperature dependence of magnetization M(T) for the sample in the temperature range $4.2 \div 1000$ K in the external magnetic field H = 1 kOe. At temperatures of $130 \div 230$ K, the Curie–Weiss behavior of magnetization is observed, i.e., the $M^{-1}(T)$ dependence is linear. As the temperature increases above ~230 K, magnetization decrease faster than 1/T, and at temperatures
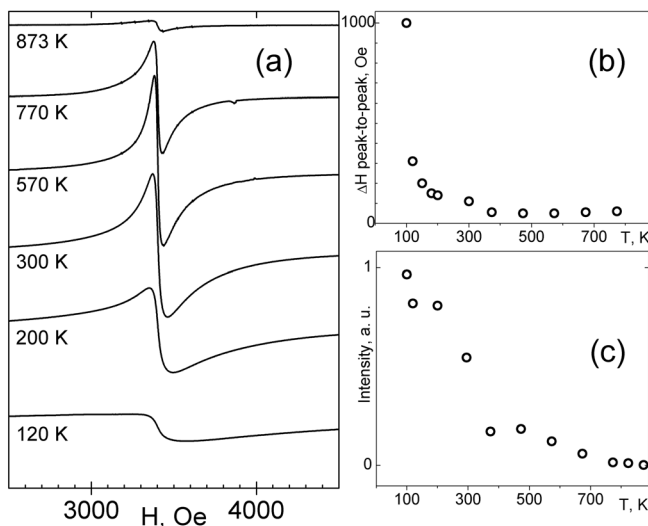
$400 \div 470$ K, it sharply drops down to ~0.25 emu/g. With a further increase in temperature, specific magnetization slightly grows attaining the maximum at T ≈ 620 K with M(T)~0.32 emu/g (inset in the Fig. 5). The temperature regions $400 \div 470$ K and $620 \div 750$ K correspond to the negative curvature of the M(T) dependence. Above ~870 K, the magnetic moment of the sample is zero within the experimental error.

The different authors observed various T_C value: 500 K,[26] 510 K,[24] or 585 K.[19] Indeed in our case, one can deduce the T_C value to be in the region of $510 \div 585$ K as the sharp magnetic moment drop appears that correlates the referred works. However, for the system under study, the magnetic moment does not completely vanish at 510 K (Fig. 5), so one should not consider this drop to be the Curie temperature of the sample containing supported ε-Fe_2O_3 nanoparticles on the silica within ~2-6 nm range. Unfortunately the temperature dependence of magnetization for ε-Fe_2O_3 nanoparticles measured before[19,26] was reported for the temperature range up to the ~600 K only.

In previous work,[24] it was reported that system of ε-Fe_2O_3 nanoparticles has the Curie temperature at 510 K while the magnetic order of the system disappears only at ~850 K as in the present work.

Detailed consideration of the data obtained allows one to suggest the ferrimagnetic order in the ε-Fe_2O_3 nanoparticles in the sample. As is known, in the case of the ferrimagnetic order, one may observe very different M(T) curves because the temperature behavior of magnetization of a ferrimagnet is determined by relative values of the exchange interactions in sublattices and their saturation magnetizations.[27] So, the sharp drop of magnetization at $400 \div 470$ K and the presence of the local maximum at T ≈ 620 K (Fig. 5) can be attributed to the variation in the ratio between the values of the exchange interaction in a ferrimagnetic particle. At the same time, the non-zero magnetic moment of the particles explains the superparamagnetic

FIG. 4. (a) ESR spectra obtained at different temperatures (indicated in the plot) for the sample; (b) temperature dependence of peak width ΔH_{pp} of the ESR signal for the sample; and (c) temperature dependence of the integral intensity of the ESR spectrum for the sample.
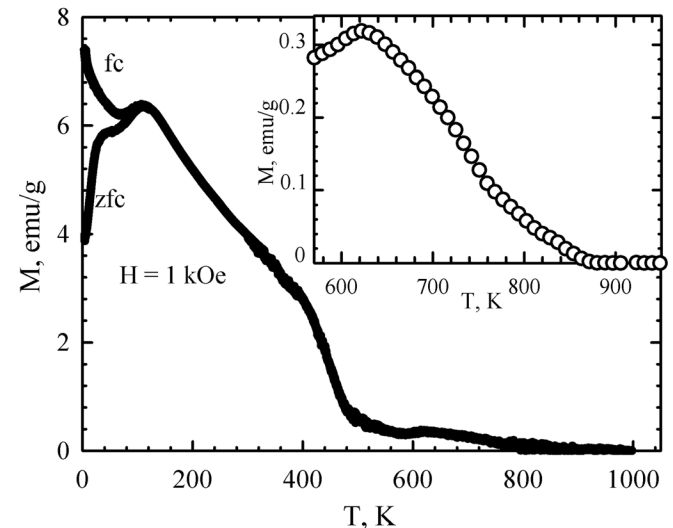
FIG. 5. Temperature dependence of the magnetic moment for the sample in an external field of 1 kOe (for the low-temperature portion, the fc and zfc regimes are indicated). The insert shows the enlarged smoothed M(T) curve in the high-temperature portion.

behavior of the system above the blocking temperature and the Curie–Weiss M(T) dependence within $130 \div 230$ K. The magnetic order vanishes at $T_C \sim 860$ K; this correlates well with the ferromagnetic resonance data showing that the sample is superparamagnetic up to T ≈ 870 K.

Taking the cell parameters for ε-Fe_2O_3 (a = 0.5098 nm, b = 0.8785 nm, and c = 0.9468 nm (Ref. 16)), one can see that there are about 1.5×10^3 iron ions in the particles with a characteristic size of ~4 nm. Meanwhile, the M(H) dependence even at T = 65 K (Fig. 3) at the relatively high magnetic fields, when the effective magnetic anisotropy of the particles is insignificant, can be satisfactorily described by the Langevin function with characteristic magnetic moment of a particle ~500 μ_B, where μ_B is the Bohr magneton. Consequently one can estimate the elemental magnetic moment to be ~0.3 μ_B, confirming the ferrimagnetic order in the particles under study. The approximate value of elemental magnetic moment is close to the one reported by M. Gish[16] 0.29 μ_B/Fe ion.

The fraction of the surface iron atoms in the ε-Fe_2O_3 particles with a size of ~3.4 nm is ~0.4. Moreover for the particles less than 2.5 nm, it is difficult to distinguish surface and volume and, hence, to speak about the presence of the long-range magnetic order. In this case, the paramagnetic behavior is observed (Figs. 2 and 3). Thus we may propose the following model of the magnetic structure of the dispersed system composed by consisting of the deposited ε-Fe_2O_3 nanoparticles. On the silica surface, there are the ε-Fe_2O_3 particles characterized by the magnetic order of different types: The largest particles have a ferrimagnetic core responsible for the superparamagnetic behavior of the system above the blocking temperature. The smallest particles, where the macroscopic magnetic moment is not formed, make the paramagnetic contribution to the temperature and field dependences of magnetization.

CONCLUSIONS

The magnetostatic and magnetoresonance properties of the monophase system consisting of the ε-Fe_2O_3 nanoparticles supported on silica with an average size of 4 nm have been studied. According to the data obtained, the system demonstrates the superparamagnetic behavior with a blocking temperature of ~120 K. The temperature behavior of magnetization allows us to make a conclusion about the existence of the ferrimagnetic order in the ε-Fe_2O_3 nanoparticles with the Curie temperature $T_C \sim 860$ K. In the low-temperature region, the paramagnetic phase makes a significant contribution, which can be attributed to paramagnetic Fe^{3+} ions in iron oxide clusters and the smallest particles

when the ferromagnetic ordering is not implemented because of an insufficient number of magnetic centers.

[1]A. H. Lu, E. L. Salabas, and F. Schuth, Angew. Chem. Int. Ed. **46**, 1222 (2007)

[2]Q. A. Pankhurst, J. Connolly, S. K. Jones, and J. Dobson, J. Phys. D **36**, R167 (2003).

[3]K. Cheng and S. Sun, Nano Today **5**, 183 (2010).

[4]H. Zeng, J. Li, Z. L. Wang, and S. Sun, Nano Lett. **4**, 187 (2004).

[5]S. Peng, C. Wang, J. Xie, and S. Sun, J. Am. Chem. Soc. **128**, 10676 (2006).

[6]S. Peng and S. Sun, Angew. Chem. Int. Ed. **46**, 4155 (2007).

[7]T. Thomson, M. F. Toney, S. Raoux, S. L. Lee, S. Sun, C. B. Murray, and B. D. Terris, J. Appl. Phys. **96**, 1197 (2004).

[8]T. Thomson, B. D. Terris, M. F. Toney, S. Raoux, J. E. E. Baglin, S. L. Lee, and S. Sun, J. Appl. Phys. **95**, 6738 (2004).

[9]G. A. Held, H. Zeng, and S. Sun, J. Appl. Phys. **95**, 1481 (2004).

[10]A. M. Testa, S. Foglia, L. Suber, D. Fiorani, Ll. Casas, A. Roig, E. Molins, J. M. Greneche, and J. Tejada, J. Appl. Phys. **90**, 1534 (2001).

[11]Y. Hou, Z. Xu, and S. Sun, Angew. Chem. Int. Ed. **46**, 6329 (2007).

[12]J. L. Dormann, F. D'Orazio, F. Lucari, E. Tronc, P. Prene, J. P. Jolivet, D. Fiorani, R. Cherkaoui, and M. Nogues, Phys. Rev. B **53**, 14291 (1996).

[13]H. Forrestier and G. C. Guiot-Guillain, C. R. Acad. Sci. (Paris) **199**, 720 (1934).

[14]E. Tronc, Ñ. Chaneac, and J. P. Jolivet, J. Sol. Stat. Chem. **139**, 93 (1998).

[15]M. Kurmoo, J.-L. Rehspringer, A. Hutlova, C. D'Orlans, S. Vilminot, C. Estourns, and D. Niznansky, Chem. Mater. **17**, 1106 (2005).

[16]M. Gich, A. Roig, C. Frontera, E. Molins, J. Sort, M. Popovici, G. Chouteau, D. Martin y Marero, and J. Nogues, J. Appl. Phys. **98**, 044307 (2005).

[17]S. Sakurai, J. Shimoyama, K. Hashimoto, and S. Ohkoshi, Chem. Phys. Lett. **458**, 333 (2008).

[18]M. Gich, C. Frontera, A. Roig E. Taboada, E. Molins, H. R. Rechenberg, J. D. Ardisson, W. A. A. Macedo, C. Ritter, V. Hardy, J. Sort, V. Skumryev, and J. Nogues, Chem. Mater. **18**, 3889 (2006).

[19]E. Tronc, C. Chanéac, J. P. Jolivet, and J. M. Greneche, J. Appl. Phys. **98**, 053901 (2005).

[20]Y.-C. Tseng, N. M. Souza-Neto, D. Haskel, M. Gich, C. Frontera, A. Roig, M. van Veenendaal, and J. Nogues, Phys. Rev. B **79**, 094404 (2009).

[21]M. Gich, A. Roig, E. Taboada, E. Molins, C. Bonafos, and E. Snoeck, Faraday Discuss. **136**, 345 (2007).

[22]G. A. Bukhtiyarova, O. N. Mart'yanov, S. S. Yakushkin, M. A. Shuvaeva, and O. A. Bayukov, Phys. Solid State, **52**, 826 (2010).

[23]G. A. Bukhtiyarova, M. A. Shuvaeva, O. A. Bayukov, S. S. Yakushkin, and O. N. Martyanov, J. Nanopart. Res., **10**, 5527 (2011).

[24]M. Popovici, M. Gich, D. Niansk, A. Roig, C. Savii, L. Casas, E. Molins, K. Zaveta, C. Enache, J. Sort, S. de Brion, G. Chouteau, and J. Nogus, Chem. Mater. **16**, 5542 (2004).

[25]G. Fazeau, V. Shilov, and J. C. Bacri, J. Magn. Magn. Mater. **202**, 535 (1999).

[26]S. Sakurai, A. Namai, K. Hashimoto, and S. Ohkoshi, J. Am. Chem. Soc. **131**, 18299 (2009).

[27]J. B. Goodenough, *Magnetism and the Chemical Bond* (Interscience Publishers, New York 1963).